PAX5 fusion genes are frequent in poor risk childhood acute lymphoblastic leukaemia and can be targeted with BIBF1120

Grazia Fazio,[a]* Silvia Bresolin,[b] Daniela Silvestri,[c] Manuel Quadri,[a] Claudia Saitta,[a] Elena Vendramini,[b] Barbara Buldini,[b] Chiara Palmi,[a] Michela Bardini,[a] Andrea Grioni,[a] Silvia Rigamonti,[a] Marta Galbiati,[a] Stefano Mecca,[a] Angela Maria Savino,[a,d] Alberto Peloso,[b] Jia-Wey Tu,[e] Sanil Bhatia,[e] Arndt Borkhardt,[e] Concetta Micalizzi,[f] Luca Lo Nigro,[g] Franco Locatelli,[h] Valentino Conter,[i] Carmelo Rizzari,[i] Maria Grazia Valsecchi,[c] Geertruij te Kronnie,[b] Andrea Biondi,[a,i] and Giovanni Cazzaniga [a,j]*

[a]Centro Ricerca M. Tettamanti, Paediatrics, University of Milano Bicocca, Monza, Italy
[b]Paediatric Haematology, Oncology and Stem Cell Transplant Division, Women and Child Health Department, Padua University and Hospital, Padua, Italy
[c]Centre of Biostatistics for Clinical Epidemiology, School of Medicine and Surgery, University of Milano-Bicocca, Monza, Italy
[d]Molecular Pharmacology Program, Memorial Sloan Kettering Cancer Center, New York, NY 10065, USA
[e]Department of Paediatric Oncology, Haematology and Clinical Immunology, Heinrich-Heine University Dusseldorf, Medical Faculty, Düsseldorf, Germany
[f]Haematology/Oncology Unit, G. Gaslini Children's Hospital, Genoa, Italy
[g]Center of Paediatric Haematology Oncology, Azienda Ospedaliero-Universitaria "Policlinico Vittorio Emanuele", Catania, Italy
[h]Department of Paediatric Haematology/Oncology and Cell and Gene Therapy, IRCCS Ospedale Pediatrico Bambino Gesù, Department of Paediatrics, Sapienza University of Rome, Rome, Italy
[i]Paediatrics, University of Milano Bicocca, Fondazione MBBM/San Gerardo Hospital, Monza, Italy
[j]Medical Genetics, University of Milano Bicocca, School of Medicine and Surgery, Monza, Italy

eBioMedicine 2022;83: 104224
Published online 16 August 2022
https://doi.org/10.1016/j.ebiom.2022.104224

Summary

Background Despite intensive risk-based treatment protocols, 15% of paediatric patients with B-Cell Precursor Acute Lymphoblastic Leukaemia (BCP-ALL) experience relapse. There is urgent need of novel strategies to target poor prognosis subgroups, like PAX5 translocated.

Methods We considered 289 childhood BCP-ALL cases consecutively enrolled in Italy in the AIEOP-BFM ALL2000/R2006 protocols and we performed extensive molecular profiling, integrating gene expression, copy number analyses and fusion genes discovery by target-capture NGS. We developed preclinical strategies to target PAX5 fusion genes.

Findings We identified 135 cases without recurrent genetic rearrangements. Among them, 59 patients (43·7%) had a Ph-like signature; the remaining cases were identified as *ERG*-related (26%), High-Hyperdiploid-like (17%), *ETV6::RUNX1*-like (8·9%), *MEF2D*-rearranged (2·2%) or *KMT2A*-like (1·5%). A poor prognosis was associated with the Ph-like signature, independently from other high-risk features.

Interestingly, *PAX5* was altered in 54·4% of Ph-like compared to 16·2% of non-Ph-like cases, with 7 patients carrying *PAX5* fusions (PAX5t), involving either novel (*ALDH18A1, IKZF1, CDH13*) or known (*FBRSL1, AUTS2, DACH2*) partner genes. PAX5t cases have a specific driver activity signature, extending to multiple pathways including LCK hyperactivation. Among FDA-approved drugs and inhibitors, we selected Dasatinib, Bosutinib and Foretinib, in addition to Nintedanib, known to be LCK ligands. We demonstrated the efficacy of the LCK-inhibitor BIBF1120/Nintedanib, as single agent or in combination with conventional chemotherapy, both *ex vivo* and in patient-derived xenograft model, showing a synergistic effect with dexamethasone.

Interpretation This study provides new insights in high-risk Ph-like leukaemia and identifies a potential therapy for targeting *PAX5*-fusion poor risk group.

Funding Ricerca Finalizzata-Giovani Ricercatori (Italian Ministry of Health), AIRC, Transcall, Fondazione Cariparo.

*Corresponding author at: Centro Ricerca Tettamanti, University of Milano-Bicocca, Via Pergolesi 33 - 20900 Monza (MB), Italy.
E-mail addresses: grazia.fazio@unimib.it (G. Fazio), giovanni.cazzaniga@unimib.it (G. Cazzaniga).

Key words: Childhood ALL; PAX5 fusion genes; Ph-like ALL; BIBF1120; Nintedanib

Research in context

Evidence before this study

The discovery of the Philadelphia-like (or BCR/ABL-like) subgroup of patients affected by acute lymphoblastic leukaemia is the most relevant recent advancement in the definition of the ALL genetic landscape, and even more relevant, a step forward in the identification of new patients' subgroups targetable with precision therapy. In addition to the pioneer studies by Mullighan's and Den Boer's groups (in 2009), we considered several independent studies which further characterized Ph-like patients and reviewed both by Pui in 2017 and Shiraz in 2020. Moreover, further new genetic subgroups of ALL emerged, with association with outcome and potential for targeting, in a continuous path for the definition of ALL heterogeneity and a chance for improving the cure rate by emerging therapies. More specifically in this context, we focused our attention on the ALL subgroup with *PAX5* gene alterations, summarized by the two most recent studies by Gu 2019 and Jung 2020, and by our own previous studies on both i) *PAX5* fusions in infant ALL patients and ii) on the functional characterization of the activated pathways downstream to *PAX5* fusions, as a potential target for therapies.

Added value of this study

In this paper, in addition to the description of the Ph-like subgroup in the Italian population of childhood ALL, we extend the genomic landscape with further details of other '-like' subgroups and additional copy number abnormalities. A main advantage of this study is the long follow up of the populations which allows a more stable outcome profile.

Compared to previously published studies, our focus on *PAX5* gene rearrangements allowed us to detail the characterization of the *PAX5* gene fusion with several different partners. Herewith, we show that *PAX5* fusion genes are more recurrent among Ph-like patients and they have their own specific signature, which is here detailed. Moreover, we show that *PAX5* fusions can be targeted by Dasatinib, Bosutinib and Foretinib, in addition to the kinase inhibitor BIBF1120/Nintedanib, which is directed against the Lymphocyte-specific tyrosine kinase (LCK), which is over-activated in PAX5 translocated cases.

Implications of all the available evidence

The *ex vivo* and *in vivo* testing of the LCK inhibitor BIBF1120/Nintedanib sustains the rationale for developing novel preclinical strategies to target *PAX5* fusion genes, a step forward in the precision medicine for childhood ALL. In the future, patients carrying *PAX5* fusions may benefit from a novel therapeutic approach.

Introduction

Despite intensive risk-based treatment protocols, 15% of paediatric patients with B-Cell Precursor Acute Lymphoblastic Leukaemia (BCP-ALL) experience disease relapse. Technological improvement progressively refined the molecular characterization of childhood ALL, identifying among other features the "Ph-like" subgroup (also known as "*BCR/ABL1*-like").[1,2] Ph-like patients are characterized by poor outcome regardless of treatment protocol, with a high incidence of relapse in children, adolescents and adult cohorts.[3,4] Ph-like ALL was also recognized as a provisional entity in the 2016 revision to the World Health Organization (WHO) classification of haematologic neoplasms[5] and there is general agreement on the importance to identify the Ph-like subtype. Those patients are characterized by recurrent molecular alterations, mainly fusion genes, classifiable as either *ABL*-class (involving *ABL1, ABL2, PDGFRA, PDGFRB, CSF1R, LYN*) or *JAK/STAT*-class (affecting *JAK2, CRLF2, EPOR*).[4,6] The pathogenetic involvement of kinase pathways sustained the use of kinase inhibitors already included in trials for Ph-positive ALL.[7,8]

In addition, other molecular lesions have been discovered in the Ph-like subgroup, whom prognostic impact still needs to be elucidated, also in association with cooperative lesions, e.g., *IKZF1*-plus profile.[9] Namely, *PAX5* gene alterations have been frequently detected in Ph-like ALL, however, their relation with the Ph-like signature, association with outcome and targeting have been poorly elucidated. The *PAX5* gene, which encodes for a B-cell related transcription factor, is altered in about 30% of BCP-ALL as being involved in deletions, amplifications, mutations and translocations that determine the formation of fusion genes encoding aberrant transcription factors.[10,11] Recently, Gu *et al.* characterized *PAX5* alterations (PAX5alt) as an heterogeneous group in childhood and adult cohorts,[12] including cases carrying either *PAX5* fusion genes, P80R variant and others, with P80R representing a subgroup with intermediate prognosis.[12,13] Importantly, the PAX5alt signature cluster is very tight and partially overlaps with

the Ph-like one, whereas *PAX5* P80R has a completely separated pattern.[12] Overall, PAX5alt and *PAX5* P80R account for 9·7% of B-other ALL and have a significant role in leukaemia initiation, prognosis and risk stratification, thus requiring an early identification and target therapy.[12]

Our previous studies, in murine pre-BI cells as well as in primary patient cells, showed that *PAX5* fusions sustain survival of leukemic cells through overexpression of the Lymphocyte kinase (*LCK*) gene[14,15] a directly repressed target of PAX5.[16] We demonstrated that LCK hyperactivation upon *PAX5* fusion expression leads to STAT5 activation and survival advantage, and that LCK phosphorylation can be specifically targeted by the kinase inhibitor BIBF1120, also known as Nintedanib (Boehringer Ingelheim, Ingelheim am Rhein, Germany),[15] a small molecule which acts as a triple kinase inhibitor with anti-angiogenic anti-tumour effect.[17] Nintedanib is approved for the treatment of patients with idiopathic pulmonary fibrosis,[18] in use in phase 3 and 4 trials for solid tumors[19] (e.g. pancreatic, hepatocellular, ovarian cancers and lung carcinomas), as well as in three clinical studies for relapsed/refractory adult AML (www.clinicaltrial.gov). It binds the ATP pocket domain of many molecules and it blocks the activity of many receptor-tyrosine kinases,[20] such as the VEGF/FGF/PDGF receptors and the non-receptor tyrosine kinases Src-family members, including LCK.[17,20]

The present study aimed at the characterization of *PAX5* rearranged cases among the Ph-like subgroup of children with BCP-ALL diagnosed in Italy. We herewith tested *ex vivo* and *in vivo* the efficacy of the LCK inhibitor Nintedanib/BIBF1120, setting the rationale for developing novel preclinical strategies to target *PAX5* fusion genes.

Methods

Patients' cohort

We considered a cohort of 289 consecutive childhood BCP-ALL cases enrolled in Italy in the AIEOP-BFM ALL2000/R2006 protocols (Eudract number: 2007-004270-43).[21] Among them, we identified 135 cases defined as "B-others" by excluding patients with the recurrent t(9;22), t(12;21), t(4;11) or t(1;19) translocations, or cases either with High Hyperdiploidy state (DNA index≥1·16) or carrying constitutional trisomy 21. To confirm that the study cohort was representative of the whole B-other population, the features of the study cohort of $N = 135$ cases were compared with the whole B-other population of 837 patients enrolled in the same period in Italy in the AIEOP-BFM ALL2000/R2006 protocols. Analyses did not reveal any difference considering gender, age or MRD stratification. Although the study cohort was, likely by chance, enriched for high-risk features (i.e., prednisone response and WBC and consequently stratification to the final High-Risk group), nonetheless, the estimated 5 years EFS did not differ between analysed and not-analysed patients (74.2±3.8 vs 76.5±1.6, respectively, $p = 0.48$) (data not shown).

Ethics

Investigation has been conducted in accordance with the ethical standards of the Declaration of Helsinki and following national and international guidelines. The study is approved by each institutional review board (Eudract number: 2007-004270-43). A written informed consent was obtained from patients or legal representatives. Regarding animal work, ethical approval was obtained by the Animal Welfare Office of the University of Milano-Bicocca prior to submit the request to the Ministry of Health. Animal testing was conducted in accordance with current European and National legislation (authorization n° 09/2018, protocol FB7CC·38 released by the Italian Minister of Health).

Gene expression profiling and Leukaemia diagnostic classification model

Patients were analysed using HG-U133 Plus 2.0 microarray (Affymetrix, Santa Clara, CA, USA) to assess Gene expression profiles. Leukaemia subtypes were classified accordingly to the previously published diagnostic GEP categories using The Diagnostic Classifier (DC) model. The model is based on all-pairwise linear classifiers for the 18 distinct classes of leukaemia, MDS and healthy control, developed for the Microarray Innovation LEukemia (MILE) study, as described in previous studies.[22] Data were normalized using Robust Multiarray Average (RMA) method using Bioconductor R package (r-package.org). ComBat function in the sva package was used to correct the batch effect of different protocol for microarray preparation. Unsupervised analyses were generated using the top 1000 variable (based on variance) probe sets and processed by t-SNE algorithm with a perplexity score of 30. Data are available at GEO (accession numbers GSE79547, GSE13164, GSE13159, GSE13204). A data-driven network inference algorithm (NetBID, https://jyyulab.github.io/NetBID/)[23] was applied to identify drivers in PAX5-translocated BCP-ALL patients, and a scalable solution of the Algorithm was used for the Reconstruction of Accurate Cellular Networks (SJARACNe).[24] The top 44 drivers for PAX5t were selected using default parameters reported in the package and p value<0·05 on the primary comparison PAX5t versus BCP-ALL excluding Ph-like/BCR-ABL-like group. Genes resulted with a positive driver activity in PAX5t by NetBID2 analysis ($p < 0.05$) were subjected to DGIdbv4.2.0 software analysis to identified drug approved interactions. Cytoscape v3.9.0 was used to build gene-drug interaction network.

Copy number alteration analysis in B-others cohort

DNA material of BM at diagnosis was available from 131/135 patients for Copy Number Alteration (CNA) analysis using Multiplex Ligation-dependent Probe Amplification (MLPA)[25] or the Affymetrix Cytogenetics Whole Genome 2.7M Array or Cytoscan-HD (Affymetrix, Santa Clara, CA) according to the manufacturer's protocol.

DNA and RNA target capture NGS analysis and bioinformatics

DNA or RNA target capture Next Generation Sequencing analysis has been performed for 86/135 patients, following a bioinformatic pipeline previously setup in our laboratory.[26] Total RNA was extracted during diagnosis from bone marrow mononuclear cells by the guanidinium thiocyanate-phenol-chloroform method and the RNA Capture 'TruSight RNA PanCancer' (Illumina, San Diego, CA, USA) was applied. If RNA was not available, we applied a DNA target panel including 17 genes, by Nextera Rapid Capture Custom panel (Illumina). We used the Illumina MiSeq platform. FASTQ files are available in the ArrayExpress database (www.ebi.ac.uk/arrayexpress) under accession number E-MTAB-11319. Fusion genes were validated by RT-PCR (experimental details are provided in Supplementary Table S7).

In vivo expansion of leukemic cells and drug experiments

Primary patient-derived xenograft (PDX) samples were obtained by intravenous injection of BM cells at diagnosis of *PAX5* translocated BCP-ALL patients into female NSG mice (NOD/SCID gamma-/- mice, Charles River Laboratories, Calco, Italy) after at least two weeks of acclimatization and then after sublethal irradiation (125 Rad, X-ray) with Radgil (Gilardoni, Mandello del Lario, Italy). Leukaemia engraftment expansion was periodically evaluated by intra-femoral BM aspiration and assessed by FACS as positive to hCD10 (eBioCB-CALLA, APC, #17-0106, RRID AB_11043552, eBiosciences, Thermofisher) and to CD19 (HIB19, FITC, #11-0199, RRID AB_10669461, eBiosciences, Thermofisher). We monitored weekly the engraftment and signs of distress or toxicity, such as shaggy fur, walking problems and weight loss (if more than 20% the animal is considered for the humanitarian end-point). At bulk disease detection of hCD10/CD19 positive cells (>10% by intra-femoral BM aspiration), we randomized mice (at least $N = 5$ for each group) and we started a daily treatment by either BIBF1120 (40 mg/kg, by oral gavage (o.g)) or dexamethasone [0·5 mg/kg, by intraperitoneal injection (i.p.)], or in combination, for 2 weeks and wash out during the weekend. No animals have been excluded. The vehicle group has been treated both by o.g. BIBF1120 vehicle (Kolliphor/ethanol/water) and by i.p. physiological solution. At the end of treatment, we sacrificed animals and analysed data in hematopoietic tissues and organs, such as Bone Marrow (BM), Peripheral Blood (PB), Spleen (SP), and meninges of Central Nervous Systems (CNS). Spleen weight was recorded prior to cell recovery. We collected the absolute number of cells for organs and we assessed the percentage of human cells (hCD10/CD19/CD45) vs. murine cells (mCD45) by FACS, to assess leukaemia engraftment (hCD45, Clone 2D1, #347464, RRID: AB_400307, BD Biosciences; mCD45, 30-F11, #12-0451, RRID AB_465668, eBioscience). According to experimental needs and international guidelines, we estimated to include $N = 5$ animals to each group (groups of animals, included in a single cage), $N = 4$ groups in each experiment, for a total of $N = 20$ animals in each experiment. The experimental staff was aware during the conduction of the experiment and analysis, not during the allocation and a strategy for potential confounders was not applied. We performed the power analyses according to Freedman, using a log-rank statistic test and the 3Rs rules. In details, the number of animals was calculated by considering either the final number of animals, the total number of events, the proportion of surviving in the control group and the estimated proportion of surviving in the experimental group, calculating a difference of 30% in survival outcome. We obtained to use 20 mice per single experiment, composed by 4 independent treatment groups of 5 mice each.

Ex vivo drug screening experiments of leukemic blasts

Ex vivo extended drug screenings were performed as previously described.[27–30] Briefly the DMSO dissolved compound library (MedChemExpress, NJ, USA) was dispensed with increasing concentrations of the inhibitors in 6 dilution steps (0.008 - 25 μM) using digital dispenser (D300e, Tecan, Männedorf, Switzerland), which ensures precise and robotic compound application in randomized fashion. Differential responses were monitored with ATP-dependent CellTiter-Glo Luminescent cell viability kit (Promega, Madison, USA) after 72 h of inhibitor exposure using Microplate reader (Spark® 10M, Tecan). Drug sensitivity scores (DSS) for the inhibitors were determined, followed by heat map visualization and unsupervised hierarchical clustering of the DSS scores were performed using R package gplots.[31]

Ex vivo apoptosis experiments of leukemic blasts in co-culture with human bone marrow stromal cells

Blasts derived from xenografts were plated on a layer of human bone marrow stromal cells (HBMS). Stromal cells were seeded at the concentration of $2x10^4$/well in MW96, three days prior to reach confluence and then leukemic blasts were plated at $2x10^5$/well in 200μl of

AIM V (ThermoFisher). At 48h we tested three different concentrations (including IC50) for each drug, in monotherapy or combination. Apoptosis/viability was evaluated by Annexin V-PE and 7-AAD staining (kit GFP CERTIFIED Apoptosis/Necrosis detection, Enzo Life Science Inc., Lausen, Switzerland) on leukemic cells positive by anti-hCD10-APC (BD Biosciences). Vincristine (stock 1mg/mL), dexamethasone (4mg/mL), L-asparaginase (kidrolase, stock 4000 IU/mL) and BIBF1120/Nintedanib (stock 10nM) were tested. In order to determine the efficacy of drug treatments and their combinations, the following parameters have been used: IC50 to determine the efficacy of drugs to inhibit the 50% of their targets and BLISS score: formula used to determine synergic (OE>EE), additive (OE=EE) or antagonist (OE<EE) activity between the drugs used in experiments Exy=Ex+Ey-(Ex*Ey), considering the expected effect (EE) of single drugs together Ex and Ey, and the Observed Effect (OE) really observed in experiments. Furthermore, we analysed data by Compusyn software, based on the Chou-Talalay's combination index theorem (CI) to evaluate the effect of interaction between n drugs: CI<1 stands for synergy, CI=1 for additivity, CI>1 for antagonism.

Phosphoflow analysis

As previously setup and validated in our lab,[15] the phosphoflow test was used to evaluate the levels of phosphorylation of PDPK1, Akt (Ser473), Akt (Thr308), S6 (S235/S236), 4EBP1 (Thr37/46), in leukemic cells (CD10+) derived from mice treated with vehicle or Nintedanib mice. After 1·5h serum starvation in X-VIVO at 37°C leukemic cells were then fixed for 10 minutes at room temperature by 1·5% PFA/mL and then permeabilized with 90% cold methanol, kept on ice for 30 minutes then washed with Staining Buffer. Further, cells were dark stained for 30 minutes at room temperature with antibodies directed to PDPK1 (Anti-PDPK1 pS241 #560092 RRID: AB_1645523 BD Biosciences), pAkt (Ser473) (Phospho-Akt Ser473 #4075 Cell Signaling), pAkt (Thr308) (Anti-Akt pT308 #558275 RRID: AB_2225329 BD Biosciences), pS6 (Anti-S6 pS235/pS236 #560435 RRID: AB_2869348 BD Biosciences) and 4pEBP1 (Phospho-4E-BP1 Thr37/46 #2846 Cell Signaling). Cells were also stained for CD10 (CD10 PE-Cy^{TM}7 #565282 RRID: AB_2739153 BD Biosciences), in order to clearly detect B leukemic cells.

FACS experiments

BD FACS CANTOII or LSRX20 FORTESSA cytometer (BD Biosciences) and FACSDiva software were used.

Statistical analysis

Analysis of clinical characteristics of patients were performed by the chi-square test for association, when appropriate. Event-free survival (EFS) was calculated from the date of diagnosis to the date of the first event. Events considered were resistance, relapse, death or second malignant neoplasms, whichever occurred first. EFS curves were estimated according to the Kaplan-Meier method, with standard errors (SE) according to the Greenwood formula; differences between groups were evaluated using the log-rank test. Cumulative incidence of relapse (CIR) curves accounting for competing events, were estimated according Kalbfleisch and Prentice and compared using the Gray test. SAS software, version 9·4, was used for analysis. Statistical analyses from *in vivo, ex vivo* and phosphoflow experiments were performed by GraphPad Prism software (ver·9); Anova and T test is shown as $*p < 0{\cdot}05$, $**p < 0{\cdot}01$, $***p < 0{\cdot}001$. Normality of phosphoflow data was demonstrated by normal distribution test (Excel). Moreover, for each experimental set of data of *ex vivo* and *in vivo* drug treatments experiments, data were analysed for D'Agostino-Pearson omnibus K2 normality test (alpha=0·05) by GraphPad Prism software (ver·9).

Role of funders

This work was supported by Ricerca Finalizzata-Giovani Ricercatori (Italian Ministry of Health) for reagents used in *ex vivo* and *in vivo* experiments. Moreover, AIRC and Transcall grants contributed to expenses for patients' data collection, molecular profiling and characterization. Fondazione Cariparo supported costs due for data analysis. The funders did not have any role nor in study design, data collection, data analyses, interpretation or writing of report.

Results

With the aim to define targetable subgroups, we considered consecutively diagnosed 289 BCP-ALL patients and defined 135 cases referred to as 'B-others' according to the workflow (outlined in figure S1) which excluded recurrent aberrations and specific gene expression signatures. B-others were scrutinized for specific GEP profiles and fusion transcripts by RNA-seq, and unsupervised t-distributed stochastic neighbour embedding (tSNE) analysis (Figure 1a) allowed to recognized several BCP-ALL subtypes based on the expression of the first 1000 most variable genes and fusion transcripts. Patients with a Ph-like profile formed the largest group of 59/135 of B-other patients. The remaining cases clustered together with known groups and were denominated accordingly.

A significant poor risk was confirmed for our Ph-like patients' cohort. In fact, Ph-like cases had a significantly inferior EFS (5-year figure (SE) of 59·9% (6·5) for Ph-like versus 85·2% (4·1) for non-Ph-like, $p = 0{\cdot}001$), mainly due to a higher CIR (Table 1; Figure 2, panel a,

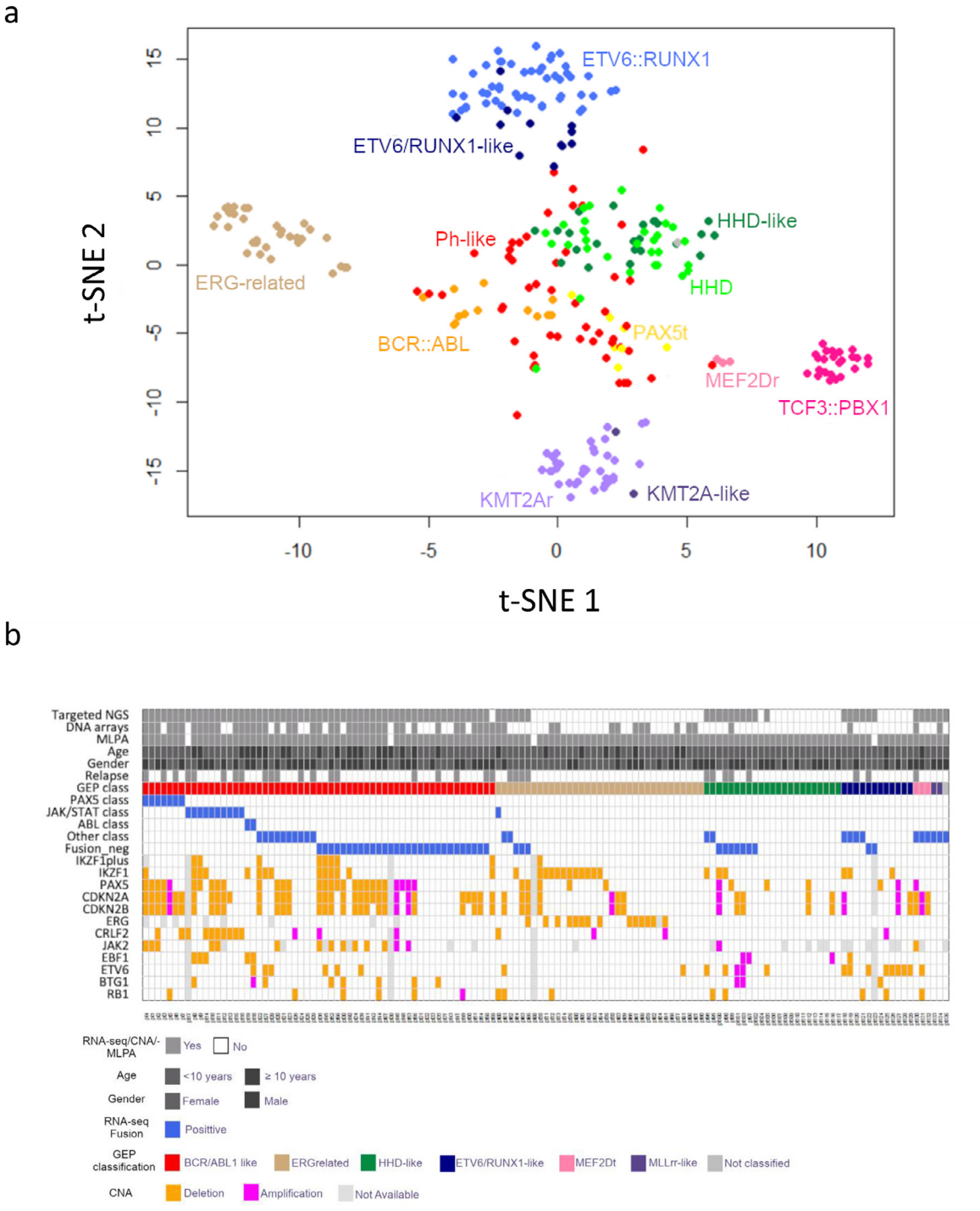

Figure 1. (a) Two dimensional tSNE plot of 289 paediatric BCP-ALL cases based on the top 1000 variable genes of gene expression data. The BCP-ALL subgroups are represented with different colours. Colour label indicated the different subgroups. Yellow highlights a subgroup of Ph-like patient carrying PAX5-translocations (PAX5t). Groups recognized as "like" cluster together with samples carrying the associated translocations, which is attributed to a similar gene expression profile. (b) Plot summarizing the molecular characterization of B-other cohort in childhood ALL: assessment of specific genetic subtypes, as reported in details in Supplementary Table S2.

	Ph-like		Non-Ph-like	
	N	%	*N*	%
Total n. of patients	59	*43·7*	76	*56·3*
GENDER				
Male	36	*61·0*	37	*48·7*
Female	23	*39·0*	39	*51·3*
p-value=0·15				
AGE				
1-5 yrs	28	*47·5*	42	*55·3*
6-9 yrs	11	*18·6*	23	*30·2*
10-17 yrs	20	*33·9*	11	*14·5*
p-value=0·02				
WBC				
<20000	25	*42·4*	47	*61·8*
20-100000	28	*47·4*	20	*26·3*
>=100000	6	*10·2*	9	*11·9*
p-value=0·04				
Prednisone RESPONSE				
Good	52	*88·1*	61	*80·3*
Poor	7	*11·9*	15	*19·7*
p-value=0·22				
MRD stratification				
Standard	15	*28·8*	17	*27·4*
Medium	28	*53·9*	38	*61·3*
High	9	*17·3*	7	*11·3*
Not known	7		14	
p-value (NK excluded)=0·60				
FINAL RISK				
Standard	14	*23·7*	16	*21·0*
Medium	31	*52·6*	43	*56·6*
High	14	*23·7*	17	*22·4*
p-value=0·89				
Non Ph-like subgroups				
ETV6::RUNX1-like			12	*15·8*
HHD-like			23	*30·3*
KMT2A-like			2	*2·6*
ERG-related			35	*46·0*
*MEF2D*r			3	*4·0*
Class-tie (not evaluable)			1	*1·3*
Events				
Resistant	0		0	
Death in Induction	1	*1·7*	0	
Relapses	20	*33·9*	12	*15·8*
- BM	*17*		*5*	
- CNS	*1*		*0*	
- BM+other	*2*		*7*	
Death in CCR	3	*5·1*	0	
- After CHEMO	2			
- After HSCT	1			
SMN	0		1	*1·3*
Alive in CCR	35	*59·3*	63	*82·9*

***Table 1*: Clinical Characteristics and outcome of Ph-like vs. non-Ph-like subgroups, in AIEOP ALL 2000/R2006.**

left and middle, $p = 0{\cdot}01$). The Overall Survival is inferior in Ph-like vs. non-Ph-like (5-year, 75·4% vs. 94·6%, $p = 0{\cdot}003$). The significantly poor EFS and OS were confirmed when excluding cases already classified as high risk (HR) ($p = 0{\cdot}02$ and $p = 0{\cdot}049$, Figure 2, panel b left and right), with a trend for higher CIR (Figure 2, panel b middle). In HR patients the 5-year EFS (SE) was 35·7% (12·8) for Ph-like vs. 76·5% (10·3) for non-Ph-like ($p = 0{\cdot}03$, Figure 2, panel c left), with a trend for a difference in CIR (50·0% (13·4) vs. 17·6% (9·6), $p = 0{\cdot}08$) (Figure 2, panel c right). Notably, the survival in Ph-like is 42·9% vs. 82·4% in non-Ph-like ($p = 0{\cdot}029$). When medium risk (MR) and standard risk (SR) patients were considered separately, the Ph-like outcome was associated with worse prognosis only in MR (60·1% vs. 85·4%, $p = 0{\cdot}02$, Supplementary Figure S2a and S2b). The EFS analysis of the most represented B-other subgroups (Ph-like, *ERG*-related, *ETV6::RUNX1*-like and HHD-like, whose clinical characteristics are described in Supplementary Table S1) confirmed that Ph-like patients show the worst outcome (Supplementary Figure S3a), even excluding HR patients (Supplementary Figure S3b). Events according to subgroups are shown in Supplementary Table S2. Of relevance, among 32/135 B-other cases experiencing relapse (23·7%), 20 were Ph-like (34%), as indicated in Table 1, and their clinical characteristics are shown in Supplementary Table S3. Moreover, a Cox model was fitted on our cohort of 135 patients; given the relatively small sample, we adjusted for the main characteristics known as generally associated to outcome. A highly significant impact on EFS was confirmed for Ph-like (hazard ratio (HR)=2·93, *p*-value=0·003) as well as for assignment to final High-Risk group (HR=2·25, *p*-value=0·03), while age and WBC at diagnosis did not have a significant impact on outcome (Table 2).

In addition, we collected data from immunophenotype analysis of the complete cohort ($N = 135$) and we classified data according to phenotype profiles, according to Ph-like signature: Non-Ph-like: pre-pre-B: 9%; call: 60%, pre-B: 18%; preB/B: 1%; Biclonal B: 4% and B-lineage: 8%; whereas Ph-like were distributed as follows: pre-pre-B: 2%; call: 81%, pre-B: 14% and B-lineage: 3%. Thus, overall, the majority of cases were classified as having call phenotype in both groups.

In Ph-like patients, CNAs were recurrent in leukaemia-associated genes, such as *CDKN2A* and/or *CDKN2B* (33·6%), *PAX5* (25·2%), *IKZF1* (24·4%), *ETV6* (15·3%), *RB1* (10%) and *CRLF2* (8·4%) (Figure 1b), with the IKZF-plus profile accounting for 7% of cases (Supplementary Table S4). The mean number of CNA events per Ph-like patient is almost double (2·77 events/pt) compared to ERG-related patients (1·53 events/pt) or non-Ph-like B-other patients overall (1·57 events/pt).

Fusion genes were identified in 30/58 (52%) Ph-like cases analysed (see heatmap of Figure 1b and Supplementary Table S4). Among those 30 fusion genes, 21

a. Ph-like vs non Ph-like: overall analysis

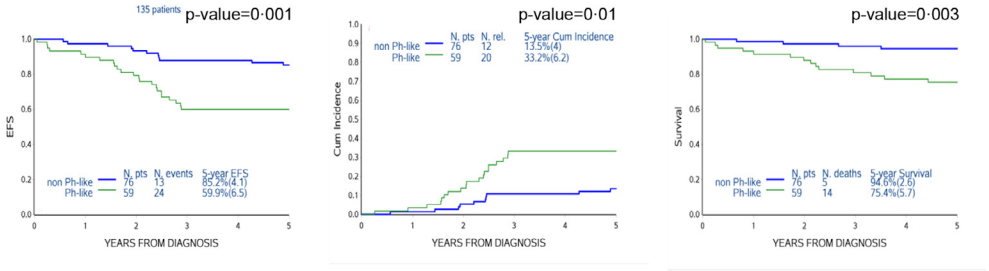

b. Ph-like vs non Ph-like: No high risk patients

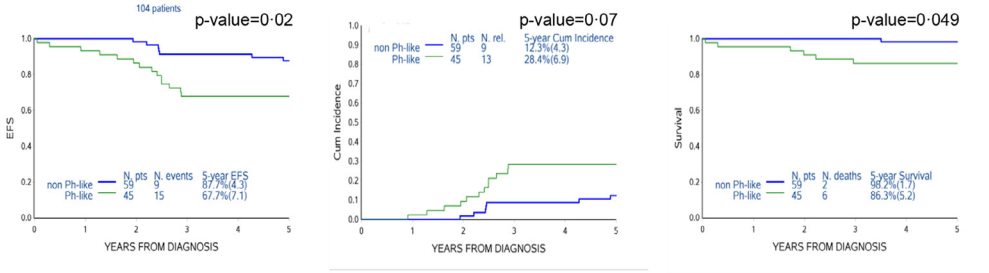

c. Ph-like vs non Ph-like: High risk only patients

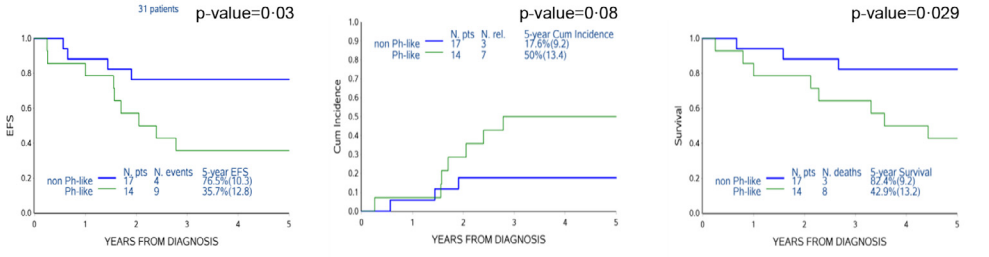

d. Ph-like patients accordingly to different class fusions

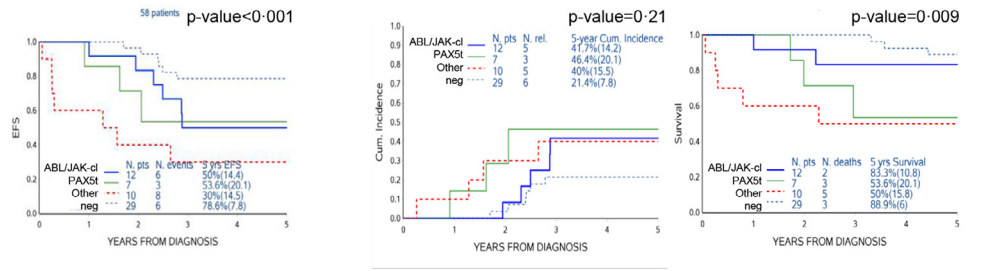

Figure 2. Outcome analysis of AIEOP B-Other cohort, in terms of EFS (on the left column) and CIR (in the middle column) and OS (in the right), comparing Ph-like vs. non-Ph-like patients overall (a), in no High Risk (b), in HR patients (c), respectively; (d) EFS, CIR and OS analyses according to the fusion classes reveal statistical significance in Ph-like cases, classified accordingly to different class fusions, such as *ABL/JAK*-class, PAX5t, other fusions and negative after NGS analysis.

	Cox model on EFS		
	Hazard Ratio	*p*-value	95% Confidence Interval
Ph-like			
Non Ph-like	1		
Ph-like	2·93	0·003	1·46-5·87
Final risk			
Non High Risk	1		
High Risk	2·25	0·03	1·09-4·67
Age at diagnosis			
1-9 years	1		
10-17 years	1·10	0·80	0·51-2·37
WBC at diagnosis			
<100000	1		
≥100000	1·16	0·78	0·42-3·21

***Table 2*: Cox model analysis on study cohort of 135 B-other patients.**

included 8 *P2RY8::CRLF2*, 7 *PAX5*-translocated cases (PAX5t), 2 *IGH::CRLF2* (by FISH), 2 *ABL*-class fusion (*EBF1::PDGFRB*) and single cases carrying either *TCF3::HLF* or *BCL9::MEF2D*. The remaining 9/30 were novel fusion genes, not previously reported in normal or cancer tissues (FusionHub database, https://fusionhub.demopersistent.com/) and classified as 'other fusions' in Supplementary Table S4. Notably, fusion genes were detected in 19/32 relapsed patients, of which 14/20 (70%) in Ph-like and only 5/12 (42%) in non-Ph-like relapsed patients. Overall, the 59 Ph-like cases could be sub grouped according to fusions as 2 *ABL*-class, 10 *JAK*-class, 7 *PAX5*-class, 9 carrying other fusions in addition to two single cases carrying either *TCF3::HLF* or *BCL9::MEF2D* and 28 remaining negative after NGS analyses. One case had no available RNA for fusion analysis but was *IKZF1*-plus as described below.

CRLF2 rearrangements were almost exclusively found in the Ph-like group (Figure 1b and Supplementary Table S4), and also the *IKZF1*-plus profile was prevalent in Ph-like cases (8/9) and associated with a poor outcome (5-year EFS (SE) 37·5% (17·1) vs 65·5% (7·0) for non-*IKZF1*-plus cases) (Supplementary Figure S4). Interestingly, also *PAX5* gene lesions were mostly associated with the Ph-like signature. Considering CNAs and translocations, the *PAX5* gene was involved in 43/131 B-other patients (32·8%), with 31/57 (54·3%) in Ph-like and 12/74 (16%) in non-Ph-like cases (Supplementary Tables S4 and S5). Notably, all the 7 PAX5t were found in the Ph-like group (Supplementary Table S5). Validation primers are reported in Supplementary Table S6. As showed in Figure 2d, EFS ($p < 0·001$) and OS ($p = 0·009$) analyses according to the fusion classes reveal statistical significance in Ph-like cases, classified accordingly to different class fusions, such as *ABL/JAK*-class, PAX5-class, other fusions and negative cases after NGS analysis. In fact, the PAX5t cases have a poor EFS, similar to *ABL/JAK*-class patients (53% and 50%, respectively) and lower than Ph-like cases negative for any fusion gene (78%). Moreover, PAX5t OS was inferior respect to *ABL/JAK*-class and negative cases (about 53% vs. 83·3% and 88·9%). However, CIR analysis was not different among the subgroups ($p = 0·21$). In details among PAX5t had 3 events out of 7, corresponding to BM relapse and they died later; among $N = 12$ *ABL/JAK*, they had one death post HSCT and 5 relapses (4 BM and 1 CNS) with only one death (the 4 non-deceased all have an adequate post-relapse follow-up).

These features of PAX5t cases prompted us to explore the feasibility of targeting patients with this aberration. By applying the NetBID2 data-driven network interference algorithms (Figure 3a), we constructed the BCP-ALL interactome and identified the hub drivers' activity (DA) based on network gene interaction on either *PAX5* translocated patients versus all BCP-ALL excluding Ph-like (Figure 3b, left column) or versus Ph-like (Figure 3b, middle column). We also assessed a Differential Expression (DE) of genes belonging to these pathways (Figure 3c). Interestingly, in the top NetBID2 drivers we identified the LCK signalling factor showing a significantly higher activity in PAX5t compared to other BCP-ALL subgroups (Figure 3d). Furthermore, analysis of LCK activity in BCP-ALL patients with known PAX5 status ($N = 131$) revealed that it is an exclusive signature of PAX5t cases, with statistically significance compared to all the categories, such as patients with amplification or deletion or being wild type for *PAX5* gene (Figure 3e). Moreover, among the 22 genes resulted with a positive driver activity in PAX5t vs. Ph-like by NetBID2 analysis ($p < 0·05$) were subjected to DGIdbv4.2.0 software analysis to identified drug approved interactions and among them we found 7 genes that can be targeted, including *LCK* by

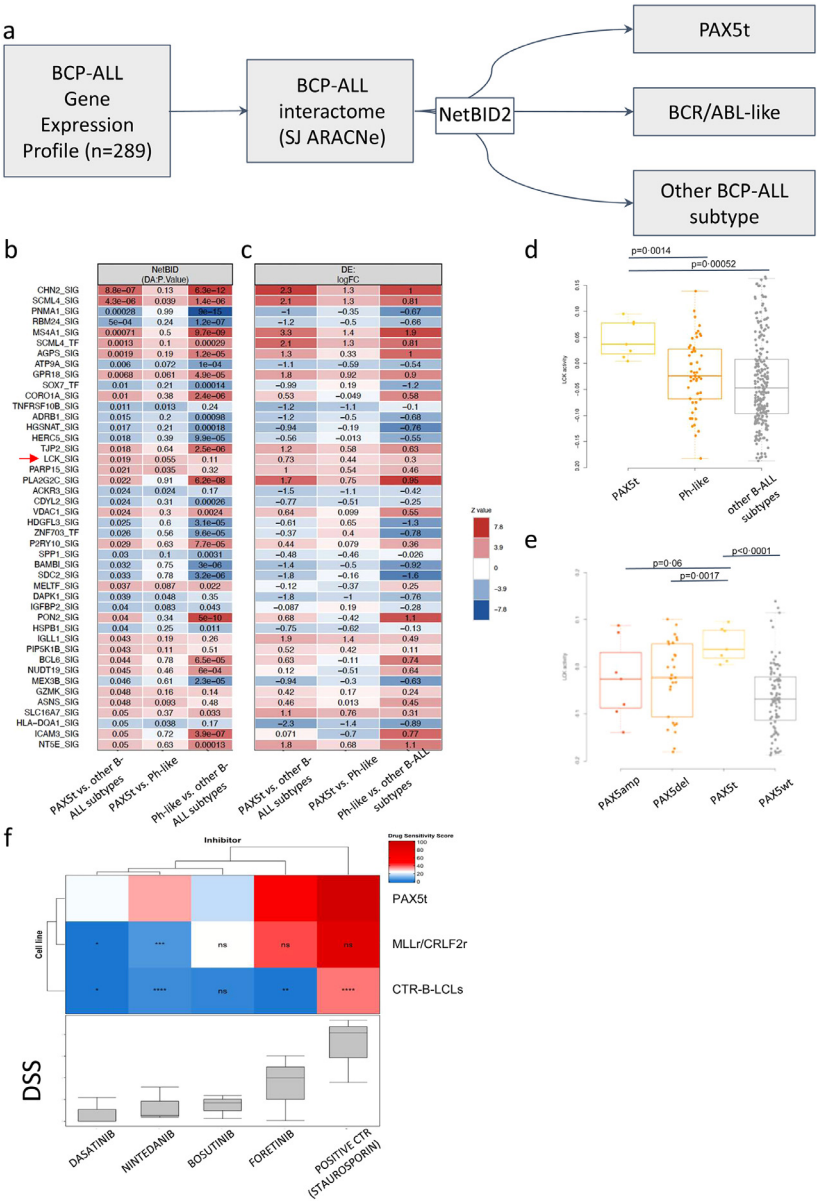

Figure 3. PAX5 translocated cases (or PAX5t) have a specific interactome signature. (a) Schema of NetBID2 analysis in BCP-ALL at diagnosis to identify driver in PAX5t BCP-ALL patients. To construct the BCP-ALL interactome the SJARCNe algorithm was employed on gene expression profiles of BCP-ALL patients (n = 289), and driver gene networks in PAX5t patients were identified in comparison with Ph-like or all other BCP-ALL subtypes. (b) Heatmap of the top 44 predicted driver's activity (DA) and (c) differentially expressed (DE) in the BCP-ALL interactome based on PAX5t patients. Drivers were ranked according to p-value. Colour code was generated by z-score. (left column= PAX5t vs. other BCP-ALL subtypes; middle column=PAX5t vs. Ph-like, right column=Ph-like vs. other BCP-ALL subtypes). (d) Boxplot of LCK activity by NetBID2 analysis of PAX5 translocated patients compared between Ph-like and all other BCP-ALL subtypes using gene expression data. p-value was calculated using Welch T-test. (e) Boxplot of LCK activity in BCP-ALL patients with known PAX5 status (N = 131). p-value was calculated by Welch t-test. PAX5amp: patients with amplification of *PAX5* gene; PAX5del: patients with deletion of *PAX5* gene; PAX5t: patients with translocation of *PAX5* gene; PAX5wt: patients with *PAX5* gene without aberrations. (f) Comparative cellular viability of different subgroups of leukemia (PAX5t, MLLr or CRLF2r) samples and control-B-lymphoblastoid cell lines (CTR-B-LCSs), measured by ATP-Glo based luminescent based assay after exposure of the depicted drugs, whereas Staurospsorin was taken as a positive control. Drug sensitivity scores (DSS) are plotted as a clustered heat map, followed by unsupervised hierarchical clustering. The horizontal and the vertical axis of the dendrogram illustrates the dissimilarity between clusters, whereas the color of the cell is related to its position along with a DSS gradient. The p-values are calculated with the one-way Anova test related to PAX5t group, **** ($p < 0{\cdot}0001$), *** ($p < 0{\cdot}001$), ** ($p < 0{\cdot}01$); * ($p < 0{\cdot}05$); ns = not significant.

Nintedanib (Supplementary Table S7 and Supplementary Figure S5a). Further, a positive enrichment of upregulated genes has been determined interacting with LCK signalling in these patients (Supplementary Figure S5b). These data pointed LCK-signalling as a potential signalling to target in this subgroup of patients. Thus, in agreement with our previous data on Pax5t targeting by the kinase inhibitor BIBF1120/Nintedanib in murine preBI cells and in primary patients' cells,[15] and sustained by independent studies in which Nintedanib is reported to be effective in LCK targeting as summarized in the Drug Gene Interaction Database (https://www.dgidb.org/genes/LCK#_interactions), we developed a LCK targeting strategy in a preclinical model of *PAX5* fusion PDX. Moreover, we applied a wider *ex vivo* drug screening with FDA-approved drugs and inhibitors in early to late clinical trials, and we selected Dasatinib, Bosutinib and Foretinib, known to be among the top 10 most potent LCK ligands, as assed by Kinome DiscoveRx study (http://www.discoverx.com/services/drug-discovery-development-services/kinase-profiling/kinomescan)[32,33] in addition to Nintedanib/BIBF1120. Here we demonstrated their potential therapeutic efficacy and specific to ($N = 3$) PAX5t cases (carrying *PAX5::AUTS2*, *PAX5::DACH2* and *PAX5::SOX5*, respectively), by evaluating the differential drug sensitivity score of PAX5t samples and including both MLLr (ALL-PO, KOPN8, RS4;11 and SEM) and CRLF2r cell lines (MUTZ5) and control B-cell lymphoblastoid cell lines (derived from healthy donors). As shown in Figure 3f, in Supplementary Figure S6 and Table S8, Nintedanib demonstrated to be the highest specific and effective compound to PAX5t, considering the statistics (One-way Anova test), compared to leukaemia cell lines and controls. We also tested other kinase inhibitors, not directly related to LCK but to BCR::ABL targeting, were not effective on PAX5t cases, whereas conventional chemotherapy drugs were effective, e.g., Dexamethasone, Vincristine among other (Supplementary Figure S6).

To investigate drug sensitivity and efficacy, we assessed apoptosis in leukemic cells. We performed *ex vivo* cell incubation by BIBF1120 alone or in combination with chemotherapeutic drugs used as standard therapy in ALL treatment protocols, such as Dexamethasone, Vincristine or Asparaginase. Figure 4 shows a representative experiment in four different *PAX5*-fusion BCP-ALL samples at 48h (2 *PAX5::AUTS2* pt.1 and pt.2, *PAX5::DACH2* pt.3 and *PAX5::SOX5* pt.4). After treatment viability has been determined, as difference from apoptosis and necrosis, by Annexin V-PE and 7-AAD staining. BIBF1120 had a synergistic effect with either Dexamethasone or Vincristine, rather than additive with Asparaginase (Combination index values are reported in Supplementary Figure S7 a-b, as Bliss score), specifically in cases carrying *PAX5* fusions, whereas it did not show any activity in *PAX5*-deleted or -wild type cases, regardless of their Ph-like profile ($N = 4$ cases, Supplementary Figure S7 panel c).

According to the synergistic effect of dexamethasone and BIBF1120 in *ex vivo* experiments, their efficacy was further assessed in the *in vivo* PDX mouse model. The BIBF1120 dose finding experiments were carried out in secondary transplants of *PAX5::AUTS2* pt.1, determining 40mg/kg as the most effective dose of BIBF1120 in absence of toxicity, phenotypic symptoms or weight loss (data not shown). Further, as schematically shown in Figure 5a, we performed secondary transplants with cells carrying either *PAX5::AUTS2* (pt.1) or *PAX5::DACH2* (pt.3). At bulk disease detection (hCD10/CD19 positive cells >10%, by BM aspiration), animals were randomized into four groups (vehicle, BIBF1120 alone, dexamethasone alone, combination) and we started treatment.

In *PAX5::AUTS2* pt.1, the daily treatment was started at day14 with 42% hCD10 positive cells mean engraftment detection in BM (ranging from 23·3 to 60·6%, Figure 5b). After two weeks, we sacrificed animals and assessed the disease levels as percentage of tumour cells in each organ, as reported in Figure 5 panels from c to g and the mean engraftment in vehicle BM was 82·6% (range 75·5-86·7%). As shown in Figure 5c, in the *PAX5::AUTS2* PDX mice we detected a mild effect in the BM of BIBF1120 alone (disease reduction of 24%, $p = 0{\cdot}057$), further enhanced by the combination with dexamethasone (-49%, $p = 0{\cdot}005$, with a mean engraftment in vehicle mice of 82·6%). In the spleen (Figure 5d and S8c), the efficacy was highly significant both for BIBF1120 (-52%, $p = 0{\cdot}025$) and the combination (-91%, $p = 0{\cdot}015$, mean engraftment vehicle 69·5%). We also observed a macroscopic effect on spleen weight decrease by the combination treatment (Figure 5e). A similar statistically significant effect was observed also in peripheral blood (Figure 5f and S8d), whilst, BIBF1120 alone showed a specific significant efficacy in CNS meninges, considering both percentages and absolute number of leukemic cells, as showed in Figure 5g and S8e, respectively. Moreover, data were further confirmed by evaluation of the tumour burden, defined as the absolute number of human CD10 positive ($hCD10^+$) leukemic cells over the total number of cells in each organ (BM, spleen, CNS and PB), as shown in Supplementary Figure S8 panel from b to e.

The efficacy of treatment was further confirmed in the *PAX5::DACH2* PDX mice. We started treatment at day21, with 15% BM Engraftment (range 10-34·3%, Figure 5h). After two weeks, the number of human leukemic cells in BM decreased of 47% using BIBF1120 alone ($p = 0{\cdot}02$ as % and $p = 0{\cdot}004$ as n° cells, Figure 5i and S8f, respectively), further diminished by the combination (-70% vs. vehicle, $p = 0{\cdot}001$ as % and $p = 0{\cdot}00001$ as n° cells, with a mean engraftment in vehicle mice of 65%, ranging from 53·3 to 70%) (Figure 5i and S8f). As shown in Figure 5l and

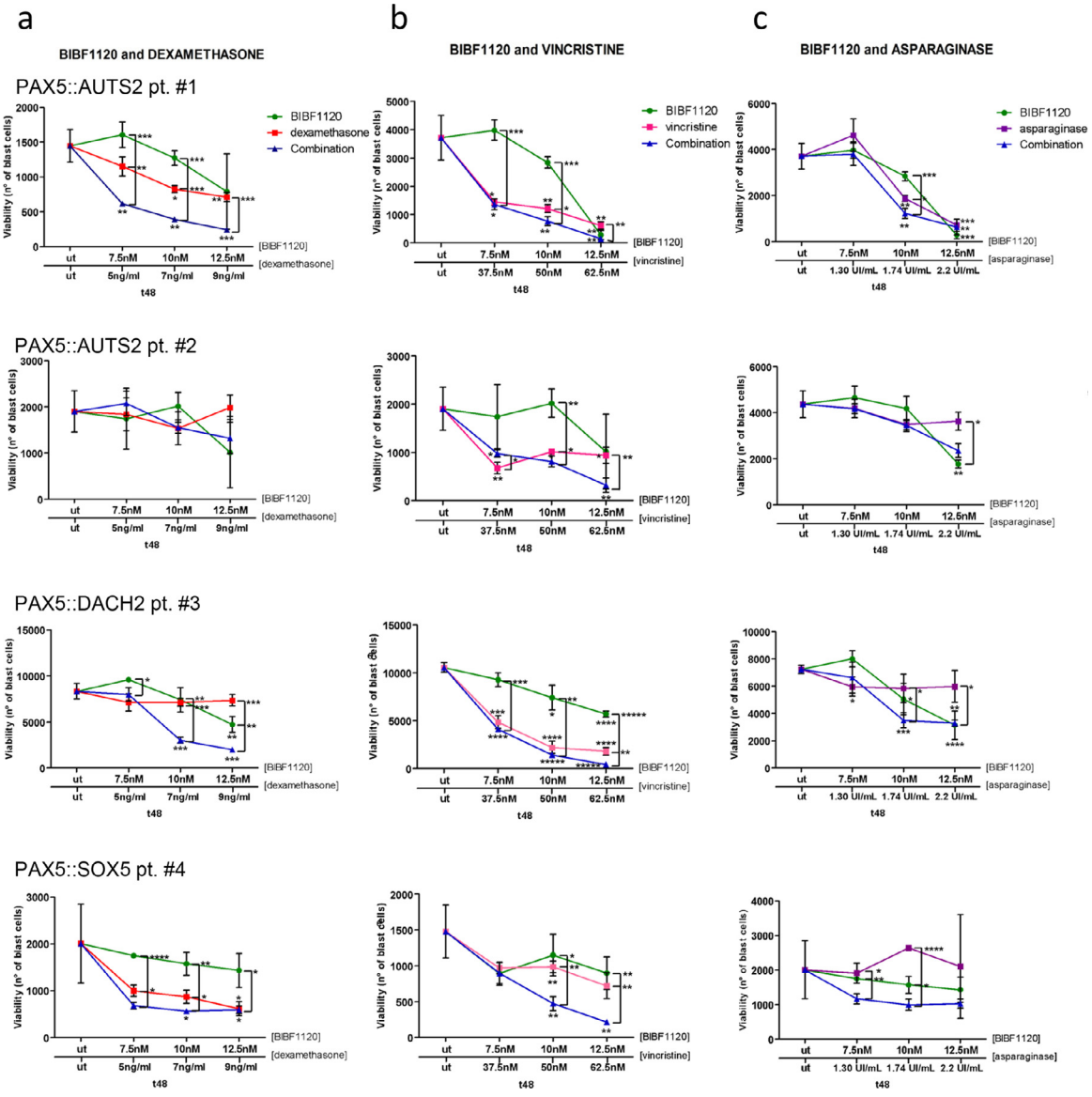

Figure 4. *Ex vivo* treatment by BIBF1120 either alone or in combination with Dexamethasone (a), Vincristine (b) or Asparaginase (c). Experiments have been performed in presence of different *PAX5* fusion genes, such as *PAX5::AUTS2* in Pt. n°1 and n°2, or alternatively carrying *PAX5::DACH2* as in Pt. n°3 or *PAX5::SOX5* in Pt. n°4. After drug treatment, viability has been determined, as difference from apoptosis and necrosis, by Annexin V-PE and 7-AAD staining. Untreated samples (ut) have been analysed as internal control.

Supplementary Figure S8g, in the spleen, the efficacy was highly significant both with BIBF1120 (-45·6%, $p = 0{\cdot}00003$ as % and $p = 0{\cdot}03$ n° cells) and the combination (-97·5% tumour burden, $p = 0{\cdot}0008$, mean engraftment vehicle 72·4%), with considerable effects on spleen weight (Figure 5m). Strikingly, BIBF1120 treatment alone showed similar efficacy in PB and CNS, with leukaemia decrease as much as -45% ($p = 0{\cdot}04$) and -76% ($p = 0{\cdot}007$), respectively. Dexamethasone alone was not effective in the BM and spleen (Figures 5i and 5l), whereas it decreased the leukaemia bulk both in PB (-65%, $p = 0{\cdot}0004$, Figure 5n) and CNS (-52·8%, $p = 0{\cdot}03$, Figure S8i). Importantly, the combination with BIBF1120 nearly achieved remission in PB (-94%, $p = 0{\cdot}0001$, Figure 5n and S8h) and it was significant in CNS (-84·7%, $p = 0{\cdot}005$, Figure 5o and S8i).

Since the AKT signalling pathway was activated downstream LCK via the PIP3 signalling pathway.[34] we hypothesised a molecular regulation mechanism involving both kinases, as depicted in Figure 6 panel a. To sustain this molecular regulation, we investigated the *in vivo* Nintedanib/BIBF1120 treatment both in four

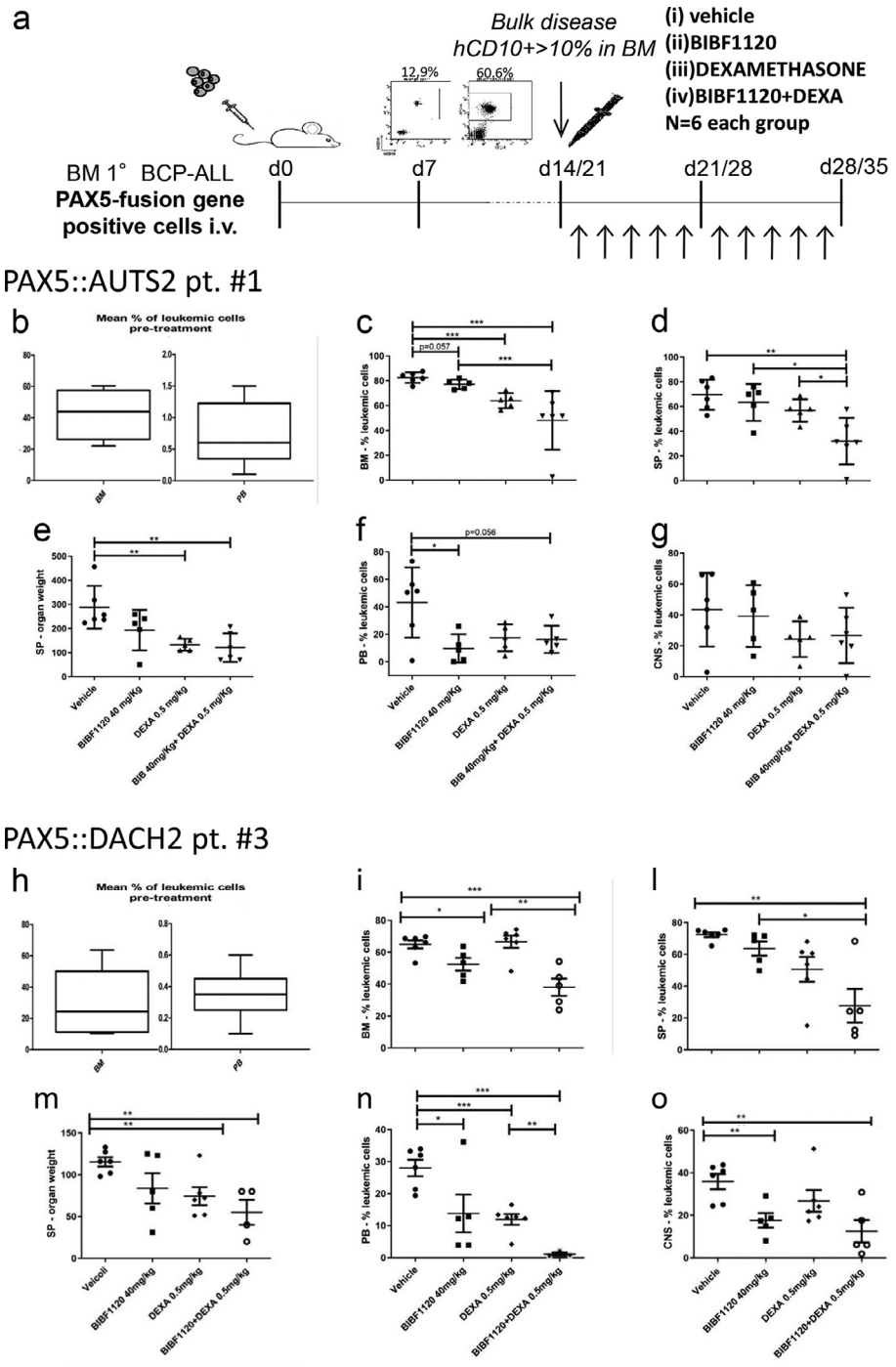

Figure 5. *In vivo* treatment by BIBF1120 either administered alone or in combination with Dexamethasone. The experimental plan is depicted in panel (a): NSG mice were transplanted with human leukemic cell carrying different PAX5 fusion genes, namely *PAX5::AUTS2* as in Pt. n°1 (panels b-g) or *PAX5::DACH2* as in Pt. n°3 (panels h-o). Human leukaemia engraftment was evaluated in hematopoietic tissues prior to start treatment in Bone Marrow and Peripheral Blood (panels b and h, in both patients, respectively) and after two weeks of treatment, in all hematopoietic organs, such as Bone Marrow for Pt.1 (panel c) and Pt.3 (panel i), in Spleen as percentage (panel d and l) and weight (panels e and m), in Peripheral Blood, f and n) and in Central Nervous System Meninges (g and o). Data are expressed as percentages of human $CD10^+$ cells. Statistical analyses have been performed by GraphPad Prism software and T test is shown as $*p < 0{\cdot}05$, $**p < 0{\cdot}01$, $***p < 0{\cdot}001$.

patients' primary cells and in *PAX5::AUTS2* mice (Supplementary Figure S9). In PDX cells phosphoflow analysis showed a marked inhibition of pAKT-Thr308 (-29%, $p < 0{\cdot}01$) and the downstream effectors pS6 (-64%, $p < 0{\cdot}001$) and 4pEBP1 (-26%, $p < 0{\cdot}05$), comparing BIBF1120 vs. vehicle group (Figure 6b). Inhibitor treatment mildly affected pAKT-Ser473 (-9%) and PDPK1 (-13%, $p < 0{\cdot}05$) phosphorylation levels. As shown in Figure 6c, we confirmed results in *PAX5::DACH2* mice, demonstrating a reliable AKT inhibition, with consistent decreased phosphorylation levels of both pAKT-Thr308 (-34%, $p < 0{\cdot}01$) and pAKT-Ser473 (-61%, $p < 0{\cdot}001$), respectively. Moreover, also PDPK1 (-37%, $p < 0{\cdot}05$), 4pEBP1 (-38%, $p < 0{\cdot}001$) and pS6 (-78%, $p < 0{\cdot}0001$) were decreased.

Discussion

After a first definition,[1,2] several studies identified the BCR/ABL1-like or Ph-like group both in paediatric and in adult cohorts of BCP-ALL, demonstrating an association with poor MRD response and overall outcome.[3] Thus, the terms '*BCR::ABL1*-like' or Ph-like have been included as provisional entity in the 2016 WHO classification of ALL.[5] In the present study, we identified and characterized the Ph-like subgroup in an AIEOP cohort of BCP-ALL patients, enrolled into the AIEOP-BFM ALL2000/R2006 protocol.[21] A Ph-like signature was defined at transcriptome level,[22] and targeted RNAseq data identified underlining molecular lesions. In addition, signatures for ERG-related, HHD-like, *ETV6::RUNX1*-like, *KMT2A*-like and *MEF2D*r subgroups were recognized.

Among B-others ALL patients, which accounted for 47% of a series of 289 new BCP-ALL diagnoses, the Ph-like profile was identified in 43·7%, corresponding to about 20% of the entire BCP-ALL cohort, in agreement with frequency previously reported.[3] The study cohort was, likely by chance, enriched for high-risk features (i.e., prednisone response and WBC and consequently stratification to the final High-Risk group but not for MRD stratification, gender or age), possibly due to the relatively limited number of samples available for analysis from the total cohort of 837 B-other patients recruited in the study period. Nonetheless, the estimated 5 years EFS did not differ between analysed and not-analysed patients (74·2±3·8 vs 76·5±1·6, $p = 0{\cdot}48$). Ph-like ALL patients are characterized by a poor outcome, independently of any other commonly used risk features, even in homogeneous risk groups, including HR patients. Importantly, the Cox model demonstrated the highly significant impact on EFS for Ph-like (hazard ratio (HR)=2·93, *p*-value=0·003) as well as for assignment to final High-Risk group (HR=2·25, *p*-value=0·03).

The Ph-like group showed molecular characteristics known to be associated to high-risk features[3,4] including the *IKZF1*-plus profile.[9] In addition, a driver fusion gene was identified in more than 50% of Ph-like cases; including the well-known *ABL*- or *JAK/STAT*-class in 20% of cases. Many studies are ongoing to target those genetic lesions mainly by deploying Tyrosine Kinase Inhibitors (TKIs) or JAK Inhibitors (JAKi)[7,35] as well as with CAR-based immunotherapy approaches.[36] These new therapeutic observations support the rationale to enrol Ph-like ALL patients in a specific clinical treatment protocol to improve treatment response with the use of TKIs.[6,8]

Here, we show that *PAX5* fusion genes are particularly recurrent among Ph-like patients: while *PAX5* lesions overall account for more than 50% of Ph-like cases, PAX5t were identified exclusively in Ph-like,[12] they have their specific signature and are associated with a poor EFS similar to *ABL/JAK*-class patients (around 50%), and an inferior OS (about 53% vs. 83%) unacceptable for childhood ALL. Likewise, we recently reported that *PAX5* fusions are recurrent and associated with poor outcome in infant ALL patients (<1 year at diagnosis), not carrying a *KMT2A/MLL* rearrangement.[37]

Importantly, and in agreement with our previous studies,[14,15] we demonstrated that *PAX5* fusions are characterized by LCK activity upregulation and are targetable by the Nintedanib/BIBF1120 inhibitor.[14,15,17,20] *Ex vivo* treatment with Nintedanib/BIBF1120 demonstrated to promote apoptosis of leukemic cells, both in monotherapy and in combination with chemotherapy agents (Vincristine, Dexamethasone or Asparaginase). Strikingly, Dexamethasone and BIBF1120 had a synergistic effect, as further assessed *in vivo* assays in PDX NSG mice with two different *PAX5* fusions (*PAX5::AUTS2* and *PAX5::DACH2*), in which we observed a significant efficacy in different organs by BIBF1120 alone and in drug combination. Overall BIBF1120 alone was more effective than Dexamethasone in reducing tumour burden. Furthermore, *ex vivo* drug screening revealed differential sensitivity of Nintedanib and Dasatinib against PAX5t leukemia samples when compared to MLLr/CRLF2r samples. Our findings are also in agreement with the role and targeting of LCK in T-ALL setting, in which they demonstrate both the role of LCK in pathogenesis and how it is possible to target with specific inhibitors such as Dasatinib and Nintedanib, through gene silencing LCK in Patient-Derived Xenograft model.[38,39]

Moreover, we demonstrated that BIBF1120 was also effective on the AKT signalling in PAX5t, by inhibiting both the pAkt-Thr308 and pAkt-Ser473 residues, essential to activate the pathway.[40] This finding reveals a role for alternative mechanisms of PAX5t leukaemia, considering that AKT is involved in apoptosis, metabolism and multidrug resistance in CLL and other malignancies.[34]

In conclusions, *PAX5* lesions are the most recurrent aberrations in Ph-like BCP-ALL, they have a specific signature and an unacceptable prognosis; PAX5t involve

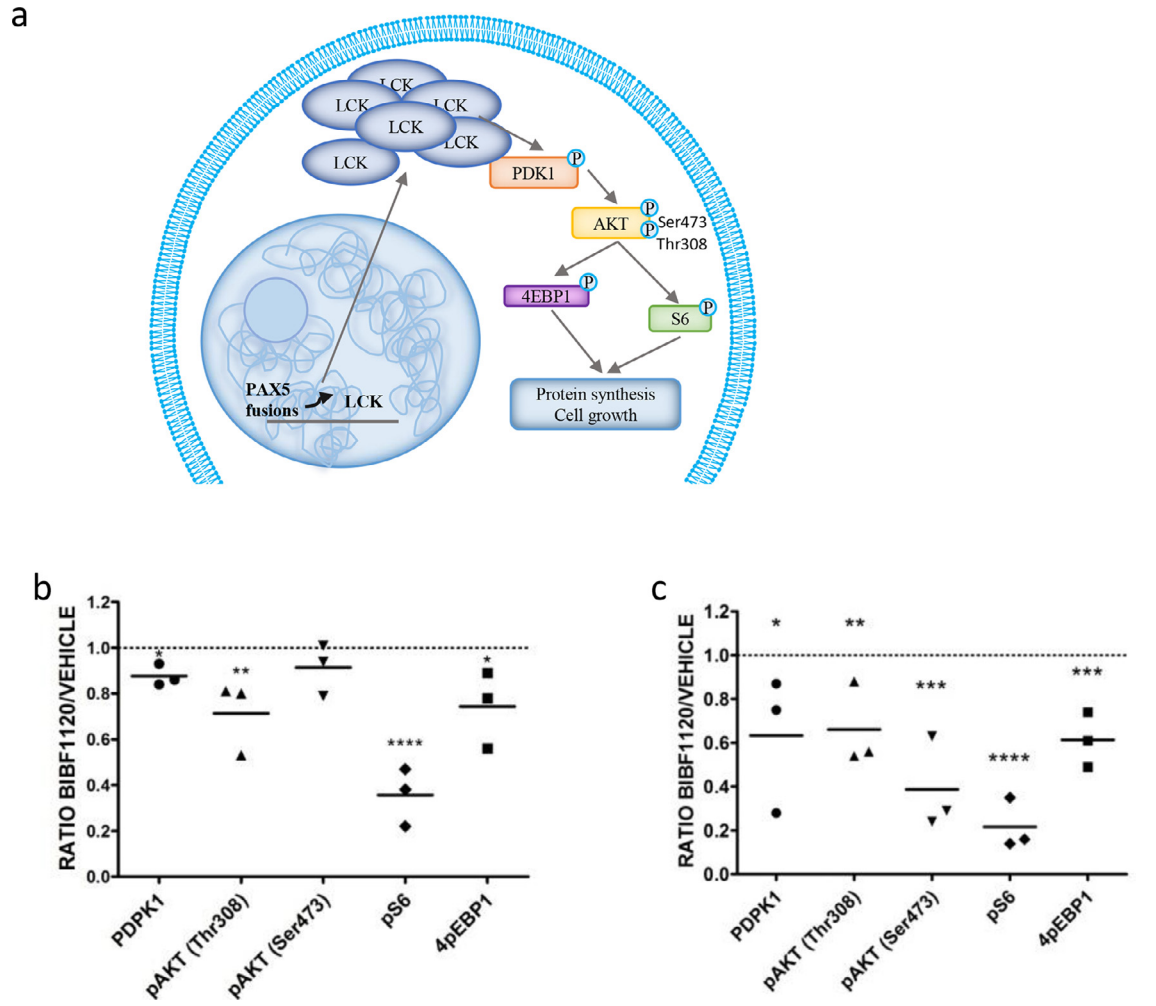

Figure 6. LCK and Akt pathway involvement in leukemic cells with *PAX5* fusion genes. (a) A schematic view of molecular hypothesised mechanism of LCK and Akt interaction. After *in vivo* BIBF1120 treatment vs. vehicle mice, in (b) pt.#1 *PAX5::AUTS2* and (c) pt.#3 *PAX5::DACH2*, respectively. PDPK1, pAKT-Ser473 and -Thr308, pS6 and 4pEBP1 are analysed by FACS. Data are expressed as ratio of Phosphorylation levels, considering vehicle phosphoprotein levels equal to 1 (dotted line) and symbols are correspondent to single BIBF1120-treated mice. Statistical analyses have been performed by GraphPad Prism software and T test is shown as $*p < 0{\cdot}05$, $**p < 0{\cdot}01$, $***p < 0{\cdot}001$.

multiple pathways that can be targeted by Nintedanib/BIBF1120. The drug could be inserted in a second line of treatment, both to allow the identification of the patient's profile and to integrate this information with the MRD analysis data. In this way it could be possible to assign these patients to an experimental group, where they receive this inhibitor in addition to the chemotherapy drugs already in use. This drug has an acceptable tolerability profile and is already approved in clinical trials for idiopathic pulmonary fibrosis by the US Food and Drug Administration (FDA) since October 2014 and by the European Medicines Agency (EMA) since January 2015, and it is tested in several cancers, with anti-angiogenic and anti-tumour effects.[17,18,20] These results strongly encourage further studies for a tailored treatment of patients with *PAX5* fusions, implementing the deployment of inhibitors in combination with chemotherapy.

Contributors

G.F., S.B. and G.C. initiated the project; G.F. and S.B. performed experiments; D.S. and M.G.V. collected patients data and performed survival analyses; E.V. and S.B. developed the signature classification; A.G. and A. P. performed bioinformatic analyses; S.R., C.S. and M. Q. performed NGS analyses and RT-PCR validation tests; C.P. and M.G. completed the CNA analyses; G.F., C.S., M.Q., C.P., M.B., S.M., A.M.S. developed the *in vivo* work; C.S. and M.Q. setup the ex-vivo and

phosphoflow experiments; B.B. performed immunophenotypic analyses; S.Bh., J.W.T. and A.B. developed and analysed drug screening; C.M., L.L.N., F.L., V.C., C. R. and A.Bi. provided access to patients' data, treated in their centres; G.F., S.B., G.tK. and G.C. analysed data and wrote the paper, with contributions from all co-authors. G.F., S.B., D.S., M.G.V., G.tk. and G.C. have verified the underlying data. All authors read and approved the final version of the manuscript.

Data sharing statement

GEP data are available at GEO (accession numbers GSE79547, GSE13164, GSE13159, GSE13204).

Target capture Next Generation Sequencing FASTQ files are available in the ArrayExpress database (www.ebi.ac.uk/arrayexpress) under accession number E-MTAB-11319.

Declaration of interests

The authors declare no competing financial interests.

Acknowledgements

This work was supported by the Italian Ministry of Health, grant Ricerca Finalizzata-Giovani Ricercatori (GR-2016-02364753 to GF, CP and MB), Associazione Italiana Ricerca per la Ricerca sul Cancro (AIRC) IG2015 no. 17593 (GC) and IG2017 no. 20564 (to AB), TRANSCALL-2 (ID 189) to AB, Fondazione Cariplo project number 2018-0339 to CP and supporting MQ fellow. Fondazione Cariparo no. 17/07_1FCR (to SB) and no. 20/12 (to BB). CS and MQ were supported from the Doctoral Program in Molecular and Translational Medicine (DIMET, University of Milano-Bicocca). We are grateful to Prof. Beppe Basso, who since the beginning was enthusiast for the contribution of gene expression profiling to the dissection of ALL, and fully supported this project. We thank the Paediatric Oncology BioBank of Padua for providing the biological material. The authors thank the BioBank of the Laboratory of Human Genetics (former Galliera Genetic Bank) member of "Network Telethon of Genetic Biobanks" (project no. GTB18001), funded by Telethon Italy, and of the EuroBioBank Network and the Assi Gulliver Associazione Sindrome di Sotos Italia provided as with specimens". The authors deeply thank the "Comitato Maria Letizia Verga" for its support with "Passaporto Genetico" project.

Supplementary materials

Supplementary material associated with this article can be found in the online version at doi:10.1016/j.ebiom.2022.104224.

References

1 Den Boer ML, van Slegtenhorst M, De Menezes RX, et al. A subtype of childhood acute lymphoblastic leukaemia with poor treatment outcome: a genome-wide classification study. *Lancet Oncol*. 2009;10(2):125–134.
2 Mullighan CG, Su X, Zhang J, et al. Deletion of IKZF1 and prognosis in acute lymphoblastic leukemia. *N Engl J Med*. 2009;360(5):470–480.
3 Pui CH, Roberts KG, Yang JJ, Mullighan CG. Philadelphia chromosome-like acute lymphoblastic leukemia. *Clin Lymphoma Myeloma Leuk*. 2017;17(8):464–470.
4 Shiraz P, Payne KJ, Muffly L. The current genomic and molecular landscape of Philadelphia-like acute lymphoblastic leukemia. *Int J Mol Sci*. 2020;21(6):2193.
5 Arber DA, Orazi A, Hasserjian R, et al. The 2016 revision to the World Health Organization classification of myeloid neoplasms and acute leukemia. *Blood*. 2016;127(20):2391–2405.
6 Izraeli S. Beyond Philadelphia: 'Ph-like' B cell precursor acute lymphoblastic leukemias - diagnostic challenges and therapeutic promises. *Curr Opin Hematol*. 2014;21(4):289–296.
7 Roberts KG, Li Y, Payne-Turner D, et al. Targetable kinase-activating lesions in Ph-like acute lymphoblastic leukemia. *N Engl J Med*. 2014;371(11):1005–1015.
8 Cario G, Leoni V, Conter V, et al. Relapses and treatment-related events contributed equally to poor prognosis in children with ABL-class fusion positive B-cell acute lymphoblastic leukemia treated according to AIEOP-BFM protocols. *Haematologica*. 2020;105(7):1887–1894.
9 Stanulla M, Dagdan E, Zaliova M, et al. IKZF1(plus) defines a new minimal residual disease-dependent very-poor prognostic profile in pediatric B-cell precursor acute lymphoblastic leukemia. *J Clin Oncol*. 2018;36(12):1240–1249.
10 Cobaleda C, Schebesta A, Delogu A, Busslinger M. Pax5: the guardian of B cell identity and function. *Nat Immunol*. 2007;8(5):463–470.
11 Mullighan CG, Goorha S, Radtke I, et al. Genome-wide analysis of genetic alterations in acute lymphoblastic leukaemia. *Nature*. 2007;446(7137):758–764.
12 Gu Z, Churchman ML, Roberts KG, et al. PAX5-driven subtypes of B-progenitor acute lymphoblastic leukemia. *Nat Genet*. 2019;51(2):296–307.
13 ung M, Schieck M, Hofmann W, et al. Frequency and prognostic impact of PAX5 p.P80R in pediatric acute lymphoblastic leukemia patients treated on an AIEOP-BFM acute lymphoblastic leukemia protocol. *Genes Chromosomes Cancer*. 2020;59(11):667–671.
14 Fazio G, Cazzaniga V, Palmi C, et al. PAX5/ETV6 alters the gene expression profile of precursor B cells with opposite dominant effect on endogenous PAX5. *Leukemia*. 2013;27(4):992–995.
15 Cazzaniga V, Bugarin C, Bardini M, et al. LCK over-expression drives STAT5 oncogenic signaling in PAX5 translocated BCP-ALL patients. *Oncotarget*. 2015;6(3):1569–1581.
16 Delogu A, Schebesta A, Sun Q, Aschenbrenner K, Perlot T, Busslinger M. Gene repression by Pax5 in B cells is essential for blood cell homeostasis and is reversed in plasma cells. *Immunity*. 2006;24(3):269–281.
17 Hilberg F, Roth GJ, Krssak M, et al. BIBF 1120: triple angiokinase inhibitor with sustained receptor blockade and good antitumor efficacy. *Cancer Res*. 2008;68(12):4774–4782.
18 Keating GM. Nintedanib: a review of its use in patients with idiopathic pulmonary fibrosis. *Drugs*. 2015;75(10):1131–1140.
19 Awasthi N, Schwarz RE. Profile of nintedanib in the treatment of solid tumors: the evidence to date. *Onco Targets Ther*. 2015;8:3691–3701.
20 Wind S, Schmid U, Freiwald M, et al. Clinical pharmacokinetics and pharmacodynamics of nintedanib. *Clin Pharmacokinet*. 2019;58(9):1131–1147.
21 Conter V, Bartram CR, Valsecchi MG, et al. Molecular response to treatment redefines all prognostic factors in children and adolescents with B-cell precursor acute lymphoblastic leukemia: results in 3184 patients of the AIEOP-BFM ALL 2000 study. *Blood*. 2010;115(16):3206–3214.
22 Haferlach T, Kohlmann A, Wieczorek L, et al. Clinical utility of microarray-based gene expression profiling in the diagnosis and subclassification of leukemia: report from the International Microarray Innovations in Leukemia Study Group. *J Clin Oncol*. 2010;28(15):2529–2537.

23 Du X, Wen J, Wang Y, et al. Hippo/Mst signalling couples metabolic state and immune function of CD8alpha(+) dendritic cells. *Nature*. 2018;558(7708):141–145.
24 Khatamian A, Paull EO, Califano A, Yu J. SJARACNe: a scalable software tool for gene network reverse engineering from big data. *Bioinformatics*. 2019;35(12):2165–2166.
25 Palmi C, Lana T, Silvestri D, et al. Impact of IKZF1 deletions on IKZF1 expression and outcome in Philadelphia chromosome negative childhood BCP-ALL. Reply to "incidence and biological significance of IKZF1/Ikaros gene deletions in pediatric Philadelphia chromosome negative and Philadelphia chromosome positive B-cell precursor acute lymphoblastic leukemia". *Haematologica*. 2013;98(12):e164–e165.
26 Grioni A, Fazio G, Rigamonti S, et al. A simple RNA target capture NGS Strategy for fusion genes assessment in the diagnostics of pediatric B-cell acute lymphoblastic leukemia. *Hemasphere*. 2019;3(3):e250.
27 Pemovska T, Kontro M, Yadav B, et al. Individualized systems medicine strategy to tailor treatments for patients with chemorefractory acute myeloid leukemia. *Cancer Discov*. 2013;3(12):1416–1429.
28 Bhatia S, Diedrich D, Frieg B, et al. Targeting HSP90 dimerization via the C terminus is effective in imatinib-resistant CML and lacks the heat shock response. *Blood*. 2018;132(3):307–320.
29 Dietrich S, Oles M, Lu J, et al. Drug-perturbation-based stratification of blood cancer. *J Clin Invest*. 2018;128(1):427–445.
30 Flumann R, Rehkamper T, Nieper P, et al. An Autochthonous mouse model of Myd88- and BCL2-driven diffuse large B-cell lymphoma reveals actionable molecular vulnerabilities. *Blood Cancer Discov*. 2021;2(1):70–91.
31 Yadav B, Pemovska T, Szwajda A, et al. Quantitative scoring of differential drug sensitivity for individually optimized anticancer therapies. *Sci Rep*. 2014;4:5193.
32 Davis MI, Hunt JP, Herrgard S, et al. Comprehensive analysis of kinase inhibitor selectivity. *Nat Biotechnol*. 2011;29(11):1046–1051.
33 Wodicka LM, Ciceri P, Davis MI, et al. Activation state-dependent binding of small molecule kinase inhibitors: structural insights from biochemistry. *Chem Biol*. 2010;17(11):1241–1249.
34 Talab F, Allen JC, Thompson V, Lin K, Slupsky JR. LCK is an important mediator of B-cell receptor signaling in chronic lymphocytic leukemia cells. *Mol Cancer Res*. 2013;11(5):541–554.
35 Boer JM, den Boer ML. BCR-ABL1-like acute lymphoblastic leukaemia: from bench to bedside. *Eur J Cancer*. 2017;82:203–218.
36 Maus MV. CD19 CAR T cells for adults with relapsed or refractory acute lymphoblastic leukaemia. *Lancet*. 2021;398(10299):466–467.
37 Fazio G, Bardini M, De Lorenzo P, et al. Recurrent genetic fusions redefine MLL germ line acute lymphoblastic leukemia in infants. *Blood*. 2021;137(14):1980–1984.
38 Serafin V, Capuzzo G, Milani G, et al. Glucocorticoid resistance is reverted by LCK inhibition in pediatric T-cell acute lymphoblastic leukemia. *Blood*. 2017;130(25):2750–2761.
39 Shi Y, Beckett MC, Blair HJ, et al. Phase II-like murine trial identifies synergy between dexamethasone and dasatinib in T-cell acute lymphoblastic leukemia. *Haematologica*. 2021;106(4):1056–1066.
40 Wei Y, Zhou J, Yu H, Jin X. AKT phosphorylation sites of Ser473 and Thr308 regulate AKT degradation. *Biosci Biotechnol Biochem*. 2019;83(3):429–435.